

ACCEPTED MANUSCRIPT

# Simultaneous de-noising and enhancement method for long-span bridges health monitoring data based on empirical mode decomposition and fractal conservation law

To cite this article before publication: Yuefeng Shao *et al* 2019 *Meas. Sci. Technol.* in press <https://doi.org/10.1088/1361-6501/ab078c>

## Manuscript version: Accepted Manuscript

Accepted Manuscript is “the version of the article accepted for publication including all changes made as a result of the peer review process, and which may also include the addition to the article by IOP Publishing of a header, an article ID, a cover sheet and/or an ‘Accepted Manuscript’ watermark, but excluding any other editing, typesetting or other changes made by IOP Publishing and/or its licensors”

This Accepted Manuscript is © 2019 IOP Publishing Ltd.

During the embargo period (the 12 month period from the publication of the Version of Record of this article), the Accepted Manuscript is fully protected by copyright and cannot be reused or reposted elsewhere.

As the Version of Record of this article is going to be / has been published on a subscription basis, this Accepted Manuscript is available for reuse under a CC BY-NC-ND 3.0 licence after the 12 month embargo period.

After the embargo period, everyone is permitted to use copy and redistribute this article for non-commercial purposes only, provided that they adhere to all the terms of the licence <https://creativecommons.org/licenses/by-nc-nd/3.0>

Although reasonable endeavours have been taken to obtain all necessary permissions from third parties to include their copyrighted content within this article, their full citation and copyright line may not be present in this Accepted Manuscript version. Before using any content from this article, please refer to the Version of Record on IOPscience once published for full citation and copyright details, as permissions will likely be required. All third party content is fully copyright protected, unless specifically stated otherwise in the figure caption in the Version of Record.

View the [article online](#) for updates and enhancements.

# Simultaneous De-noising and Enhancement Method for Long-span Bridges Health Monitoring Data Based on Empirical Mode Decomposition and Fractal Conservation Law

Yuefeng Shao <sup>a, b</sup>, Changqing Miao <sup>a, b, \*</sup>, Bowen Li <sup>a, b</sup>, Qiande Wu <sup>a, b</sup>

<sup>a</sup> Key Laboratory of Concrete and Prestressed Concrete Structures of Ministry of Education, Southeast University, Nanjing, P.R. China

<sup>b</sup> School of Civil Engineering, Southeast University, Nanjing, 211189, P.R. China

**Abstract:** This paper introduces a new signal-filtering, which is aimed at processing long-span bridges structural health monitoring (SHM) data based on empirical mode decomposition (EMD) and fractal conservation law (FCL). The long-span bridges SHM data is selected from vertical vibration data of Runyang Bridge main girder. The key idea of this paper is to enhance the frequency amplitude of target signal and at the same time to weaken the signal noise brought about surroundings by combining methods as EMD and FCL after confirming long-span bridge natural frequency by vibration EMD operation consists of EMD of vibration data, selection of effective intrinsic mode functions (IMFs) and effective IMFs recombination. FCL theory will be applied on filtering function to process effective IMFs in the frequency domain before recombination. This theory is based on a partial differential equation modified by a nonlocal fractional anti-diffusive term of lower order. Effect of EMDFCL filter is compared with EMD method, FCL method and filter strategy that combined EMD and low-pass filtering respectively. Results show that EMDFCL filter outperforms the other signal filtering methods in natural frequency recognition of long-span bridge SHM data. In particular, the bridge natural frequencies distinguished by EMDFCL match well with the calculated frequencies and original fingerprint.

**Keywords:** Empirical Mode Decomposition (EMD), Fractal Conservation Law (FCL), Structural Health Monitoring (SHM) data filtering, long-span bridge, Simultaneous De-noising and Enhancement

## 1. Introduction

As the developing of modern concepts for monitoring programs of bridge structures [1], it has arrived at a consensus that monitoring programs are necessary due to the uncertainties in environmental and mechanical conditions, material properties, loading history and so on. Structural health monitoring (SHM) data de-noising is a major challenge in measurement and estimate processes. Noise removal is an important topic in instrumentation and measurement domains where the challenge is to preserve the signal of structures while removing the noise signal [2]. Efficient de-noising strategy aims at reducing uncertainties of the SHM data and improve their quality. A

---

\*corresponding author: Changqing Miao. E-mail address: chqmiao@163.com.

1  
2  
3  
4  
5  
6  
7  
8  
9  
10  
11  
12  
13  
14  
15  
16  
17  
18  
19  
20  
21  
22  
23  
24  
25  
26  
27  
28  
29  
30  
31  
32  
33  
34  
35  
36  
37  
38  
39  
40  
41  
42  
43  
44  
45  
46  
47  
48  
49  
50  
51  
52  
53  
54  
55  
56  
57  
58  
59  
60

variety of noise reduction methods have been developed mostly based on the model-based methods, transform domain approaches and adaptive filtering [3]. For the non-stationary signals such as SHM vibration data and earthquake signal, linear methods such as Wiener filter are not suitable. David L. Donoho proposed soft-thresholding based on wavelet method to process those non-stationary signals [4]. But the wavelet approach has a limit that the basic functions and decomposition level are stationary, which means that different wavelet functions and decomposition level need be selected to filter different real signals.

During the late 1990s, Huang introduced the algorithm called empirical mode decomposition (EMD), which is widely used today to analyze the non-stationary and non-linear data [5]. EMD strategy adaptively decomposes signals into a series of “well-behaved” oscillatory components called intrinsic mode functions (IMF). It has been shown that based on partial reconstruction of relevant modes, EMD filters signals in an adaptive way [6]. With this adaptive feature, EMD tool was widely applied to process the non-stationary signals such as de-noising and frequency estimation in measurements domains [7]. In 2004, Wu and Huang researched statistical significance of IMFs by studying the statistical characteristics of uniformly distributed white noise, and each mode could be classified based on its energy-density spread function [8]. Based on energy-density spread function, probability density functions of IMFs was proposed, and relevant modes of IMFs was selected to achieve partial reconstruction to remove the noise from the signal [3]. The other filter strategies about correlation-based threshold to discriminate between relevant and irrelevant IMFs was proposed by Zheng Hongmei [9] and Chatlani Navin [10].

Fractal method is widely used in SHM datum analysis, Ebrahimkhanlou Arvin [11, 12] used multifractal fractal method to analyze crack image in crack patterns identification and damage assessment of concrete structures. Fractal conservation law (FCL) is firstly introduce by A.C. Fowler [13] to describe morphodynamics of sand dunes. And P. Azerad [14] used this algorithm to analyze electrocardiogram signal. Then, Meng Fanlei [15] applied FCL to extract seismic wave signal. Those researches showed that this method can preserve low frequencies, amplify medium frequencies and eliminate high frequencies. That is to say, FCL method can eliminate high frequencies noise effectively, but it cannot deal with the low-frequency noise.

However, the bridge SHM data is greatly affected by environmental factors, which makes the monitoring data in different environments have obvious differences. And the amount of data is very large. As the reason of that filtering effect of wavelet-based methods is influenced by the choice of wavelet function and decomposition level. It may seem redundant and complicated if we choose the appropriate wavelet function and decomposition level when processing every data. The EMD method with higher self-adaptability has a problem of mode mixing [16], which makes the bridge information and high frequencies noise appear in the same order IMF. Due to the characteristic of simultaneous high frequencies de-noising and enhancement of medium and low frequency signals, FCL method is a good strategy to overcome the defect of EMD method.

The outline of this paper is as follows. Description of the FCL is given in Section

2. Section 3 illustrates the filtering method of EMDFCL and the control groups filter. Comparison on performance metrics of different filters is presented and the discussed in Section 4. Finally, Section 5 concludes the paper with a summary.

## 2 A fractal conservation law

In this section, we present the basic theory and numerical computation scheme of the FCL used in the filter.

### 2.1 Basic theory

FCL is based on the partial differential equation (PDE) of Cauchy problem. To use a linear PDE, which includes two antagonistic terms: a usual diffusion and a nonlocal fractional anti-diffusive term of lower order, FCL is used to simultaneous noise reduction and enhancement of signals [14]. This linear PDE is:

$$\begin{cases} \partial_t u(t, x) - a \partial_{xx}^2 u(t, x) + b I_\lambda [u(t, \cdot)](x) = 0 & t \in (0, T), \quad x \in R, \\ u(0, x) = u_0(x) & x \in R, \end{cases} \quad (1)$$

where  $T$  is any given positive time,  $u(t, x)$  is the filtered signal and  $u_0$  is the original signal, which is involved with noisy signal,  $a, b$  are positive constants, and  $I_\lambda$  is a fractional operator defined as formula (2) for  $\lambda \in (1, 2)$ , then we get an explicit nonlocal formula:

$$I_\lambda [\varphi](x) = \alpha_\lambda \int_R \frac{\varphi''(x - \xi)}{|\xi|^{\lambda-1}} d\xi \quad (2)$$

where  $\alpha_\lambda$  is a suitable constant.

Then we can obtain Riemann Liouville definition of the fractional derivative [17] by replacing the limit of integration  $R$  with  $(0, +\infty)$  as follows:

$$\frac{1}{\Gamma(2-\lambda)} \int_0^{+\infty} \frac{\varphi''(x-\xi)}{|\xi|^{\lambda-1}} d\xi = \frac{d^{\lambda-2}}{dx^{\lambda-2}} \varphi''(x) = \frac{d^\lambda}{dx^\lambda} \varphi(x) \quad (3)$$

where  $\Gamma$  is the Euler function.

### 2.2 Numerical computation Scheme

We present the numerical computation scheme based on fast Fourier transform (FFT), which is an efficient algorithm to compute discrete Fourier transform, to solve equation (1) as follows:

$$\begin{cases} \frac{dU(t, \omega)}{dt} - 4\pi^2 a \omega^2 U(t, \omega) + b F [I_\lambda (u(t, \omega))] = 0 \\ F(u(0, x)) = U_0(\omega) \end{cases} \quad (4)$$

$$I_\lambda [\varphi](x) = C_\lambda \int_R \frac{\varphi(x+z) - \varphi(x) - \varphi'(x) \times z}{|z|^{1+\lambda}} dz \quad (5)$$

where  $F[u(t, x)] = U(t, \omega)$ ,  $F[u(0, x)] = U_0(\omega)$ ,  $F$  represents the Fourier transform,  $\lambda \in (1, 2)$ ,

$C_\lambda$  is a constant, which can be absorbed in  $b$ .

The equation (2) can be transformed into equation (5) by using Taylor-Poisson formula and Fubini's Theorem [15]. Replacing  $\varphi(x)$  with the vibration time history signal  $u(t, x)$ , we present the Fourier transform of  $I_\lambda$  as follows:

$$F[I_\lambda(u(t, x))] = \int_R \frac{F(u(x+z)) - F(u) - F(u') \times z}{|z|^{1+\lambda}} dz = \phi(\omega) \times U(t, \omega) \quad (6)$$

According to the time shifting and differentiation properties of the Fourier transform and Euler formula, we obtain:

$$\phi(\omega) = \int_R \frac{e^{2i\pi\omega z} - 1 - 2i\pi\omega z}{|z|^{1+\lambda}} dz = \int_R \frac{\cos(2\pi\omega z) - 1}{|z|^{1+\lambda}} dz + i \int_R \frac{\sin(2\pi\omega z) - 2\pi\omega z}{|z|^{1+\lambda}} dz \quad (7)$$

There exit two positive values of  $a_l$  and  $b_l$ , so that

$$\phi(\omega) = -a_l |\omega|^\lambda + ib_l \omega |\omega|^{\lambda-1} \quad (8)$$

The derivation process in formula (8) comes from the work [18], which provides some useful theoretical results on nonlocal conservation law. Hence, according to (4), (6), and (8), we obtain an ordinary differential equation with the solution:

$$U(t, \omega) = e^{(-t(4\pi^2 a \omega^2 - b a_l |\omega|^\lambda + i b b_l \omega |\omega|^{\lambda-1}))} \times U_0(\omega) = K(t, \omega) \times U_0(\omega) \quad (9)$$

$$|K(t, \omega)| = K_{a,b}^\lambda(t, \omega) = e^{-(4\pi^2 a \omega^2 - b |\omega|^\lambda)} \quad (10)$$

Equation (10) is the filter in the frequency domain. It is remarkable that the constant  $a_l$  is absorbed in  $b$ . Besides,  $t$ , which can be fixed at 1 to facilitate the calculation, is in the upper bound limit on time  $T$  in equation (1).

To transform equation (10) based on FFT, we deduce that the solution of equation (2) has to satisfy the equation (11):

$$u(t, x) = k(t, x) * u_0(x) \quad (11)$$

where  $*$  represents convolution,  $k(t, x) = F^{-1}(K_{a,b}^\lambda(t, \omega))$  is the kernel function of the operator  $I_\lambda - \partial_{xx}^2$ ,  $4\pi^2 \omega^2$  corresponds to diffusive operator ( $-\partial_{xx}^2$ ),  $-|\omega|^\lambda$  corresponds the fractional operator ( $I_\lambda$ ), parameters  $a$  and  $b$  represent the local diffusion and nonlocal anti-diffusion respectively. The main function, which includes local diffusion and nonlocal anti-diffusion, reduces noise and enhances contrast of the signal respectively. The filter function  $K_{a,b}^\lambda$  is drawn in Fig. 1.

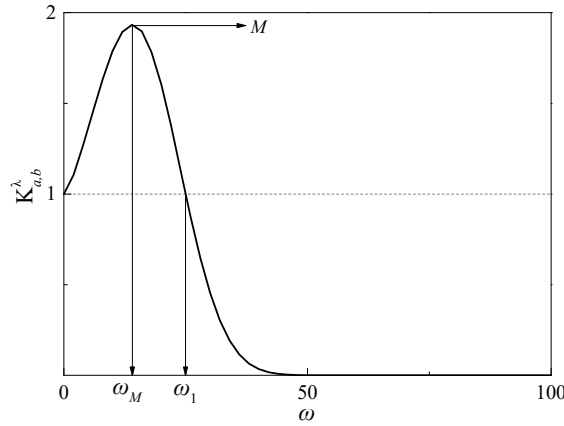


Fig. 1. Behavior of  $K_{a,b}^{\lambda}$  with  $4\pi^2a=0.01$ ,  $b=0.05$ , and  $\lambda=1.8$

### 2.3 Determination of parameters

In this section, parameters ( $a$ ,  $b$ , and  $\lambda$ ) determination is discussed, which correspond the de-noising ability and contrast enhancement. Showing in Fig. 1, those parameters can be determined by the threshold frequency ( $\omega_1$ ), the frequency of extreme point ( $\omega_M$ ), and maximum of  $K_{a,b}^{\lambda}$  ( $M$ ).

$$\omega_1 = \left( \frac{b}{4\pi^2 a} \right)^{\frac{1}{2-\lambda}} \quad (12)$$

$$\omega_M = \left( \frac{\lambda b}{8\pi^2 a} \right)^{\frac{1}{2-\lambda}} \quad (13)$$

$$M = K_{a,b}^{\lambda}(\omega_M) = e^{4\pi^2 a \times \left( \frac{\lambda b}{8\pi^2 a} \right)^{\frac{2}{2-\lambda}} \times \left( \frac{2}{\lambda} - 1 \right)} \quad (14)$$

where  $\omega_1$  controls the frequency range and satisfies  $K_{a,b}^{\lambda}(\omega_1)=1$  and  $K_{a,b}^{\lambda}(\omega) < 1$  for  $\omega > \omega_1$ ,  $M$  is larger than 1 with  $0 < \lambda < 2$ ,  $\omega_1/\omega_M = (2/\lambda)^{1/(2-\lambda)}$ .

In the actual situation, we can give the fixed value of  $\omega_1$  and  $M$ . Then, the ratio  $b/a$  can be deduced by the values  $\omega_1$  and  $\lambda$ . Using this ratio and equation (14), we can get the parameters  $a$  and  $b$ . Parameter  $a$  monitors the de-noising intensity and controls the Laplacian term. While, parameter  $b$  enhances the contrast of signal and controls the anti-diffusive term, which has the opposite behavior to the Laplacian term.

### 3. Filtering mechanism for long-span bridge

In this section, 4 different filtering methods are compared. Those signals are mainly selected from the SHM data of Runyang Bridge.

#### 3.1 information of Runyang bridge

Runyang bridge, which connects Zhenjiang City and Yangzhou City, is composed of south branch suspension bridge and north branch cable-stayed bridge. The south branch suspension bridge is a single-span, double-hinged and simply supported steel box girder bridge with a main span of 1490m. EMDFCL filtering method is verified by

the vibration data of the main girder vibration monitoring subsystem of Runyang south branch suspension bridge SHM system. The vibration data in October 2014 is selected as research object. The sampling frequency is 20 Hz and the sampling points are 72000. The arrangement of accelerometers for the main girder of Runyang Bridge is shown in Fig.2. there are 18 sensors installed in upstream and downstream of the bridge. Because of the excessive data, only the data from 0:00-1:00 on October 8 are illustrated.

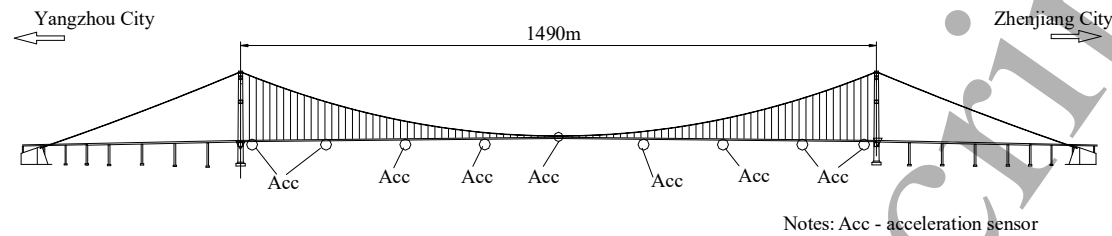


Fig.2 Arrangement of Acceleration Sensors for Runyang Bridge

To determine the band-pass frequency and truncation frequency of the filter, we refer to the nature frequency of Runyang Bridge [19, 20], and it is shown in Table1:

Table1 Nature frequency of Runyang Bridge

Mode No.	Frequency by SSI (Hz)	Mode description
1	0.122	Symmetric bending
2	0.144	Anti-symmetric bending
3	0.166	Symmetric bending
4	0.181	Anti-symmetric bending
5	0.239	Symmetric bending
...	...	...
11	0.4598	Symmetric bending

As shown in Table1, the first order symmetric vertical bending frequency of Runyang Bridge is 0.122Hz, and the 11th order symmetric vertical bending frequency is 0.4598Hz. To cover all the nature frequencies of bridge effectively, the band-pass frequency and the truncation frequency are 0.81Hz and 1Hz respectively.

### 3.2 EMDFCL filter

#### (1) EMD algorithm

In 1998, Huang proposed Empirical Mode Decomposition (EMD) to analyze data from non-stationary and non-linear systems. Through this method, the Intrinsic Mode Functions (IMFs) of the signal  $u(t)$  are obtained using the following steps [5]:

- 1) Identify all the extrema locations of the signal  $u(t)$ .
- 2) Use local spline interpolation to create the upper envelope line  $e_{\max}(t)$  and the lower envelope line  $e_{\min}(t)$ .

- 3) Calculate the local mean  $m(t) = \frac{e_{\max}(t) + e_{\min}(t)}{2}$ .

- 4) Subtract the local mean from the signal  $u(t)$  to obtain the “modulated oscillation”  $h(t) = u(t) - m(t)$ .

- 5) If  $h(t)$  satisfies the IMF requirements, set  $C_i(t) = h(t)$ , ( $i \in [1, n]$ ) as the IMF,

else set  $u(t) = h(t)$  and return to Step 1 ( $n$  is the loop counts of the Step 6 ).

6) Subtract these IMFs from the signal  $u(t)$ , so that  $u(t) = u(t) - C_i(t)$  and return Step 1.

7) Stop the sifting process when the residual  $r_n(t)$  from Step 6 becomes a monotonic function.

Finally, we obtain the equation:

$$u(t) = \sum_{i=1}^n C_i(t) + r_n(t) \quad (15)$$

The IMF requirements mentioned above are following:

1) The number of extrema and zero-crossings must either equal or differ at most by one in the whole data set.

2) The mean value of the envelope line defined by the local maxima and the local minima is zero at any point.

## (2) FCLEMD method

The EMD algorithm decomposes the signal  $u(t)$  into a set of IMFs with distinct time scale. The decomposition is based on the local time scale of  $u(t)$ , and yields adaptive basis functions. The intrawave frequency modulation of IMF can identify the different frequency of the signal. This advantage can help us to identify and remove the invalid frequency range. Moreover, the FCL can de-noise and enhance the signal further. The main steps are following:

1) Decompose the signal  $u(t)$  to obtain the IMFs by using the EMD algorithm.

2) Select the valid IMFs by identifying the PSD of every IMF (Screen out the IMF, of which frequency is lower than 0.1Hz). This screening frequency can be obtained in three ways: determined by structural basic natural frequency, structural modal analysis of finite element model and empirical estimation based on similar structures. The basic natural frequency of Runyang Bridge, which has been fully researched, is used to determine this screening frequency in this paper.

3) Transform the valid IMFs selected in step 2 into the frequency domain from time domain by FFT.

4) De-noise and enhance the IMFs simultaneously by the filter function (9) in frequency domain, then transform them back to the time domain by IFFT.

5) Recompose the valid IMFs as the valid signal  $u_v(t)$ .

In the EMDFCL method, power spectral density (PSD) analysis is applied to ascertain minimum frequency, which is used to filter IMFs of Runyang Bridge vertical acceleration. The representative signal IMF and its PSD is shown in Fig.3 to Fig.7 as follows:

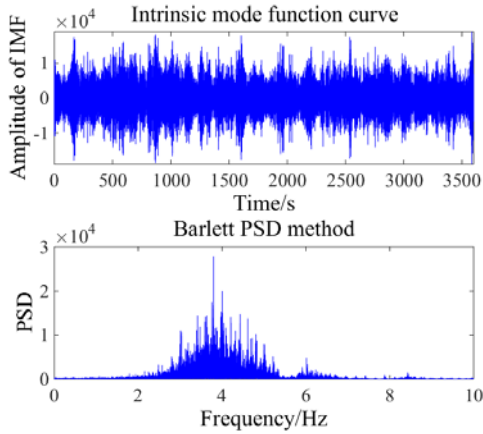


Fig.3 1st order IMF and PSD diagram

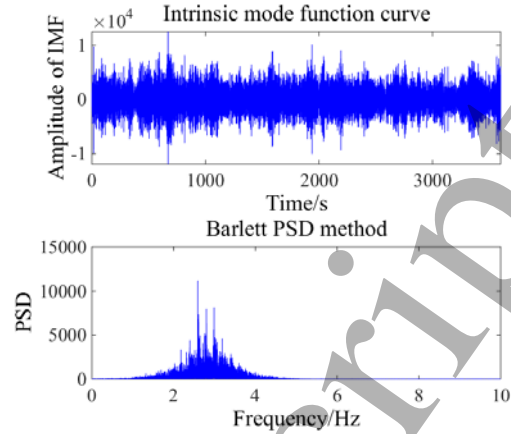


Fig.4 2nd order IMF and PSD diagram

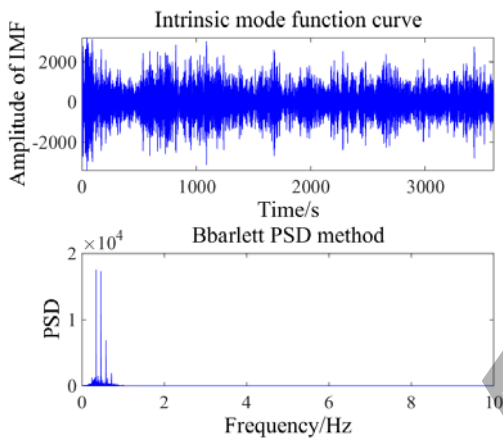


Fig.5 5th order IMF and PSD diagram

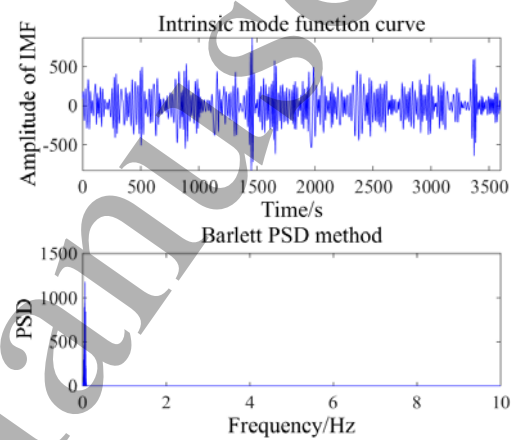


Fig.6 9th order IMF and PSD diagram

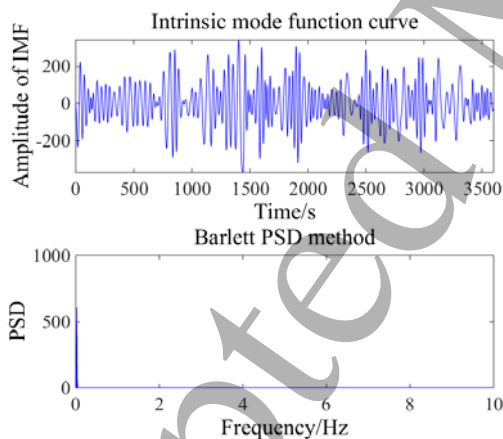


Fig.7 10th order IMF and PSD diagram

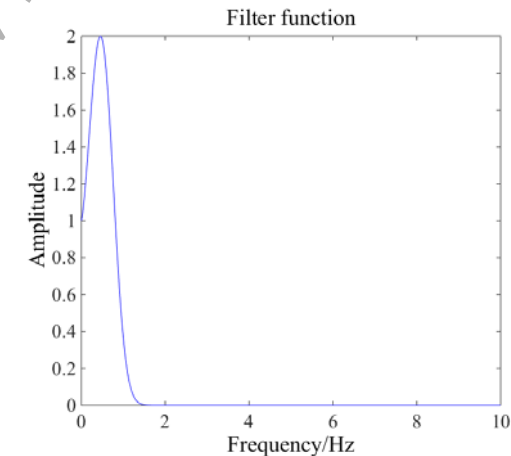


Fig.8 Transform Domain Filter

$$\text{Function } K_{a,b}^{\lambda},$$

$$4\pi^2 a = 10.02, b = 9.01, \lambda = 2$$

In Fig.3-Fig.7, as rising of IMF order, signal main frequency range decreases in IMF power spectral density analysis. Among them, 1st order IMF frequency range is among 3-5Hz. The 2nd order IMF frequency range is among 2-3.5Hz. The 5th order IMF frequency range is among 0-1Hz. The 9th order IMF frequency range is among 0-0.13Hz. The 10th order IMF frequency range is among 0-0.03Hz. As the 1st order vertical nature frequency of Runyang Bridge is 0.122Hz, first 9 orders IMFs are

remained to reduce the influence of low frequency noise.

Those remained IMFs are dealt with FCL to achieve de-noising and enhancement of signal in different frequency dimension. In this procedure, filter functions are shown in equation (9)-(13). In the equation,  $M=2$ ,  $4\pi^2a=10.02$ ,  $b=9.01$ ,  $\lambda=2$ , and the function is shown in fig7. Then, the filtering signal is obtained by recombination of those IMFs.

### 3.3 signal processing

The other four filter method is used as the contrast to the EMDFCL filter. Filtering effect of different methods is judged by comparison of Runyang Bridge nature frequency identification. The flow chat of total 5 filter methods is shown as follows:

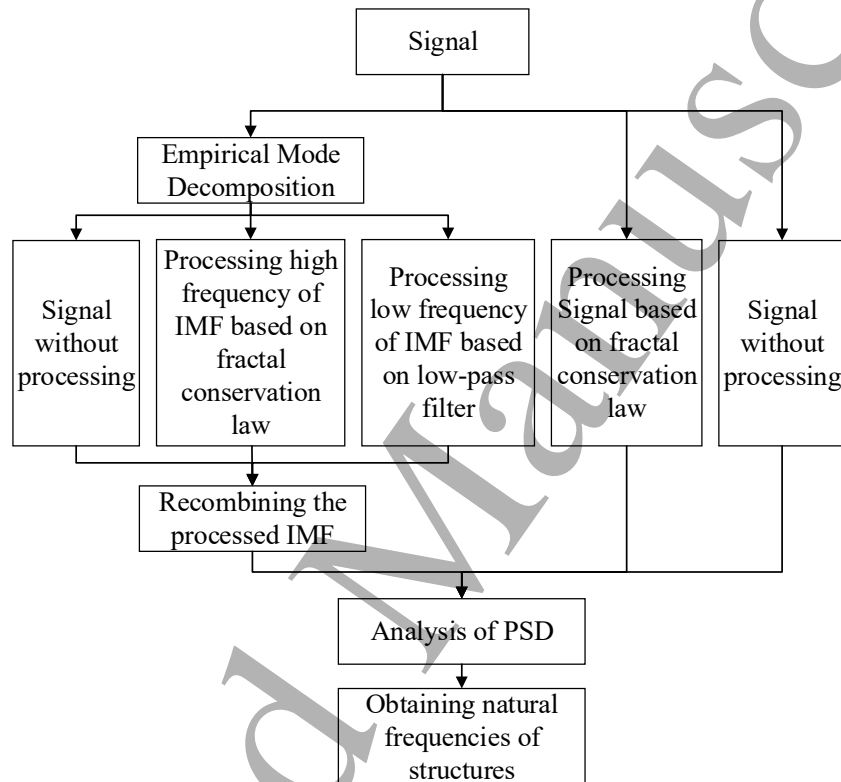


Fig.9 Flow chart of signal processing

Fig.9 shows processing of EMDFCL method and other four control group methods. Those five methods are introduced as follows:

- 1) Original signal is the first control group.
- 2) Process the signal through only EMD method: the low frequency noise will be eliminated as the recombination of IMFs.
- 3) Process the signal through EMDFCL filter.
- 4) Process signal through Only FCL method.
- 5) Replace FCL method with low-pass filter in the EMDFCL method.

The effect of filtering signals, which is processed by the methods mentioned above, is estimated by frequency order identified degree through power spectrum density analysis. And the signals filtered by the five methods above are shown as following:

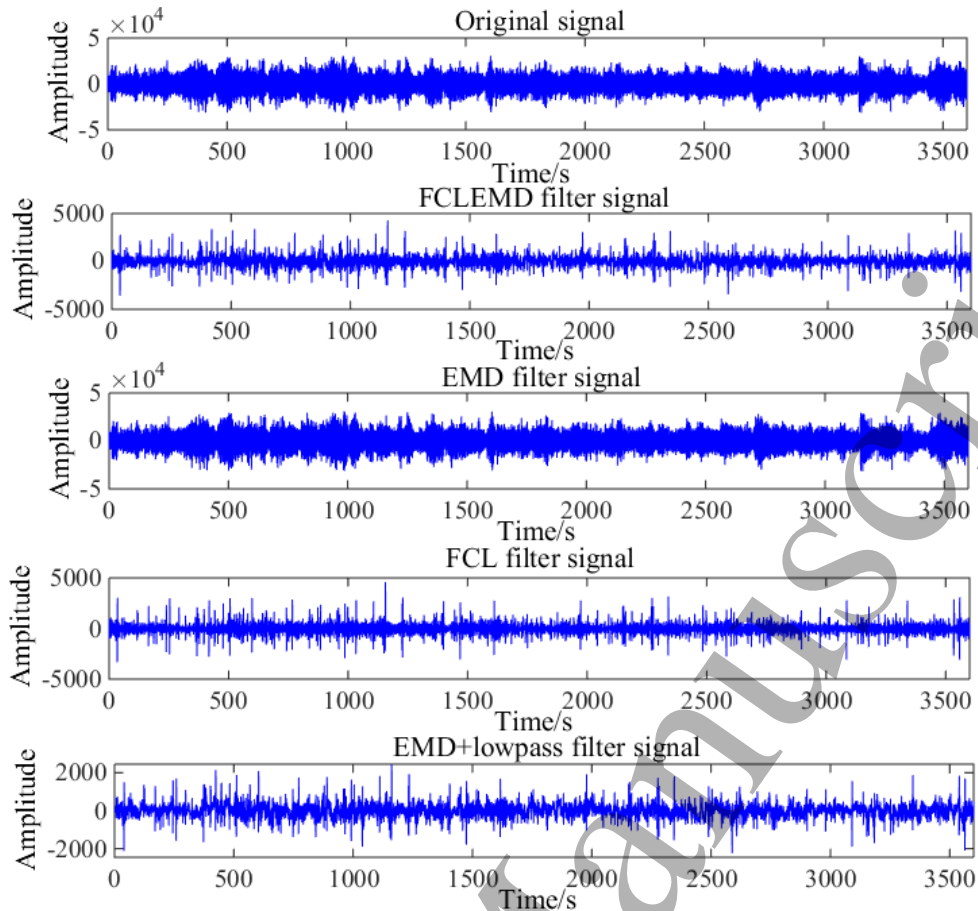


Fig.10 original signal and filter signals

After EMD processing, it can be found that the amplitude of high frequency vibration is much larger than that of low frequency vibration. As shown in Fig.10: the high frequencies of the original vibration signal and the EMD-processed signal are not filtered, so the amplitudes of those two signals (the 1st and the 3rd) are obviously larger than the signals processed by the other three methods. Comparing these three high-frequency components eliminated signals (the 2nd, the 4th and the 5th), the amplitudes of signal processed by two FCL related methods are about twice as much as that obtained by EMD-Lowpass method. This phenomenon is consistent with the enhancement effect of signal amplitude in target frequency band by using FCL method.

#### 4. Performance metrics

Power spectral density (PSD) analysis is done to distinguish the frequency order of five signals mentioned above. The PSDs of those five signals are shown as Fig.11 to Fig.15.

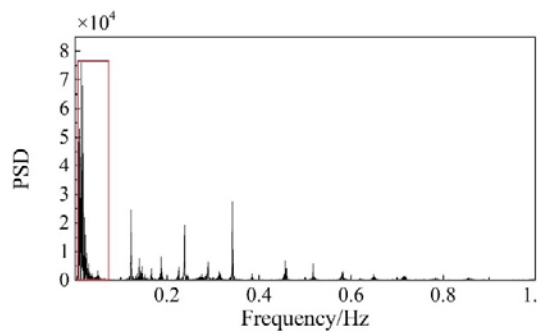


Fig.11 original signal PSD

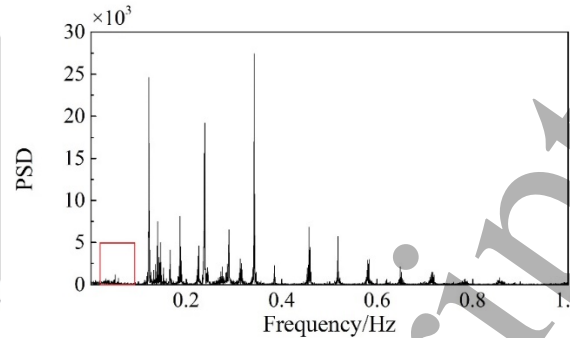


Fig.12 signal PSD of only EMD

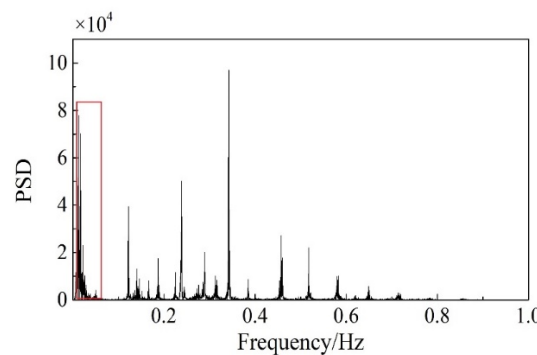


Fig.13 signal PSD of only FCL

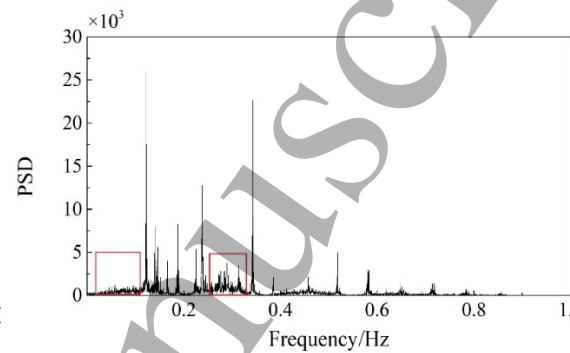


Fig.14 signal PSD of EMD and low-pass filter

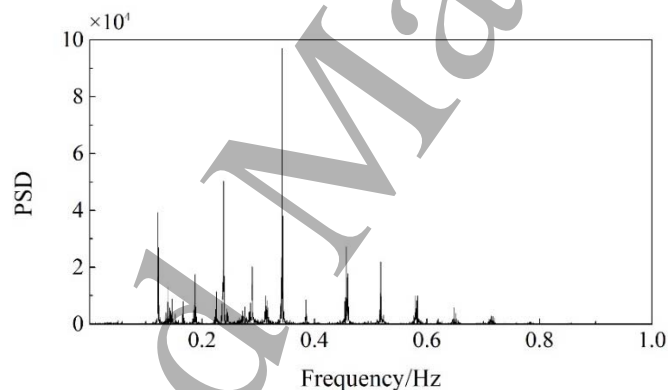


Fig.15 signal PSD of EMDFCL filter

As shown in the PSD of original vibration: Because of low frequency noise in signals, which is shown in the red box in Fig.11, bridge natural frequency recognition is difficult. Those difficulties including two aspects: 1) Low frequency noise brings about barriers and difficulties in recognition of the first order natural frequency. 2) PSD amplitude of bridge natural frequency is too small to distinguish, which makes some orders of bridge natural frequency be ignored.

In the only EMD methods, the frequency order could be recognized, but the residual low-frequency noise still has some influence on the first-order frequency identification (shown in the red box in Fig.12).

The only FCL processing method enlarges the amplitude of bridge natural frequency in PSD, but it presents poor performance in controlling low-frequency noise. As shown in the red box in Fig.13, this defect will bring about barriers in first order frequency identification.

With the processing of EMD and low-pass filter, the peak value of bridge natural frequency between 0.2Hz and 0.4Hz cannot be distinguished, which make those orders of bridge frequency cannot be recognized. And the influence of low frequency noise has not been completely eliminated (shown in the red box in Fig.14).

As shown in the Fig.15: after the processing of EMDFCL filter, the signal recognition degree of each frequency peak is distinct, and the influence of low frequency noise has been completely eliminated.

Using EMDFCL filter to distinguish the vibration data of Runyang Bridge, the comparison of recognized bridge natural frequencies, bridge calculated frequencies [19, 20] and the original bridge fingerprint [21] are exhibited in Table.2:

Table.2 Rcognized natural frequencies, calculated frequencies, original fingerprint of Runyang

Order	Mode description	Bridge		
		calculated frequencies (Hz)	original fingerprint (Hz)	recognized frequencies (Hz)
1	1st-order positive symmetric vertical bending of main girder	0.1250	0.1221	0.1217
2	1st-order anti-symmetric vertical bending of main girder	0.1426	0.1440	0.1403
3	2nd-order positive symmetric vertical bending of main girder	0.1696	0.1685	0.1664
4	2nd-order anti-symmetric vertical bending of main girder	0.1900	0.1880	0.1875
5	1st-order positive symmetric torsion of main girder	0.2383	0.2398	0.2258
6	3rd-order positive symmetric vertical bending of main girder	0.2418	-	0.2386
7	3rd-order anti-symmetric vertical bending of main girder	0.2921	0.2759	0.2894
8	1st-order anti-symmetric torsion of main girder	0.2925	0.3098	0.3133
9	4th-order positive symmetric vertical bending of main girder	0.3469	-	0.3422
10	4th-order anti-symmetric vertical bending of main girder	0.4031	-	0.3850

11	5th-order positive symmetric vertical bending of main girder	0.4609	0.4598	0.4570
----	--	--------	--------	--------

As shown in Table.2: compared the recognized signal processed by the EMDFCL filter with the calculated frequencies and the original fingerprints of Runyang Bridge, the three kinds of bridge natural frequencies have high matching degree. Some natural frequency orders, which are not recorded in the original fingerprints, can be distinguished by data processing of EMDFCL filter. Through this method, the original fingerprint parameters of bridges can be update with the analysis of SHM data.

## 5. Conclusion

In this paper, a new filtering strategy for SHM data is presented. The filtering combines methods as EMD and FCL. EMDFCL filtering simultaneously exhibits de-noised and enhanced performance compared with the classical filters and some other EMD-based filtering strategies. This method can filter low frequency noise by EMD and the recombination of valid IMFs. In this procedure, the effective IMFs being selected on the basis of the minimum frequency, which is determined by basic natural frequency of long-span bridge. Without the influence of low frequency noise, the FCL, which makes bridge nature frequency distinguishable in PSD analysis, is used to filter the high frequency component and to enhance signal frequency between nature frequency bandwidth of bridge. With the verification by extensive SHM data of Runyang Bridge, identified frequencies of vibration data filtered via EMDFCL method match well with the finite element modal parameters and original fingerprint of Runyang Bridge. In short, EMDFCL filter is an effective method to process the SHM data of long-span bridge.

## Acknowledgements

This research has been supported by the National Natural Science Foundation of China under grant number 51778135, Aeronautical Science Foundation of China under grant number 20130969010, the National Natural Science Foundation of Jiangsu Province, China, the Fundamental Research Funds for the Central Universities and Postgraduate Research & Practice Innovation Program of Jiangsu Province under grant No. KYCX18\_0113 and KYLX16\_0253.

## Reference

- [1] D.M. Frangopol, A. Strauss, S. Kim, Use of monitoring extreme data for the performance prediction of structures: General approach, *Engineering Structures*, 30 (2008) 3644-3653.
- [2] D. Dey, B. Chatterjee, S. Chakravorti, S. Munshi, Importance of denoising in dielectric response measurements of transformer insulation: An uncertainty analysis based approach, *Measurement*, 43 (2010) 54-66.
- [3] A. Komaty, A.-O. Boudraa, B. Augier, D. Dare-Emzivat, EMD-based filtering using similarity measure between probability density functions of IMFs, *IEEE Transactions*

- 1  
2  
3 on Instrumentation and Measurement, 63 (2014) 27-34.
- 4 [4] D.L. Donoho, De-noising by soft-thresholding, IEEE transactions on information  
5 theory, 41 (1995) 613-627.
- 6 [5] N.E. Huang, Z. Shen, S.R. Long, M.C. Wu, H.H. Shih, Q. Zheng, N.-C. Yen, C.C.  
7 Tung, H.H. Liu, The empirical mode decomposition and the Hilbert spectrum for  
8 nonlinear and non-stationary time series analysis, in: Proceedings of the Royal  
9 Society of London A: mathematical, physical and engineering sciences, The Royal  
10 Society, 1998, pp. 903-995.
- 11 [6] E.H. Krishna, K. Sivnai, K.A. Reddy, Empirical Mode Decomposition based  
12 Adaptive Filtering for Orthogonal Frequency Division Multiplexing Channel  
13 Estimation, International Journal of Engineering-Transactions A: Basics, 30 (2017)  
14 1517-1525.
- 15 [7] K. Khaldi, M.T.-H. Alouane, A.-O. Boudraa, A new EMD denoising approach  
16 dedicated to voiced speech signals, in: Signals, Circuits and Systems, 2008. SCS 2008.  
17 2nd International Conference on, IEEE, 2008, pp. 1-5.
- 18 [8] Z. Wu, N.E. Huang, A study of the characteristics of white noise using the empirical  
19 mode decomposition method, in: Proceedings of the Royal Society of London A:  
20 Mathematical, Physical and Engineering Sciences, The Royal Society, 2004, pp. 1597-  
21 1611.
- 22 [9] H. Zheng, C. Dang, S. Gu, D. Peng, K. Chen, A quantified self-adaptive filtering  
23 method: Effective IMFs selection based on CEEMD, Measurement Science and  
24 Technology, (2018).
- 25 [10] N. Chatlani, J.J. Soraghan, EMD-based filtering (EMDF) of low-frequency noise  
26 for speech enhancement, IEEE Transactions on Audio, Speech, and Language  
27 Processing, 20 (2012) 1158-1166.
- 28 [11] A. Ebrahimkhanlou, A. Farhidzadeh, S. Salamone, Multifractal analysis of two-  
29 dimensional images for damage assessment of reinforced concrete structures, in:  
30 Sensors and Smart Structures Technologies for Civil, Mechanical, and Aerospace  
31 Systems 2015, International Society for Optics and Photonics, 2015, pp. 94351A.
- 32 [12] A. Ebrahimkhanlou, A. Farhidzadeh, S. Salamone, Multifractal analysis of crack  
33 patterns in reinforced concrete shear walls, Structural Health Monitoring, 15 (2016) 81-  
34 92.
- 35 [13] A.C. Fowler, Evolution equations for dunes and drumlins, Revista de la Real  
36 Academia de Ciencias Exactas, Físicas y Naturales, Serie A. Mat., 96 (2002) 377-387.
- 37 [14] P. Azerad, A. Bouharguane, J.-F. Crouzet, Simultaneous denoising and  
38 enhancement of signals by a fractal conservation law, Communications in Nonlinear  
39 Science and Numerical Simulation, 17 (2012) 867-881.
- 40 [15] F. Meng, Y. Li, N. Wu, Y. Tian, H. Lin, A fractal conservation law for simultaneous  
41 denoising and enhancement of seismic data, IEEE Geoscience and Remote Sensing  
42 Letters, 12 (2015) 374-378.
- 43 [16] G. Gai, The processing of rotor startup signals based on empirical mode  
44 decomposition, Mechanical Systems and Signal Processing, 20 (2006) 222-235.
- 45 [17] I. Podlubny, Fractional Differential Equations, to Methods of Their Solution and  
46 Some of Their Applications, Fractional Differential Equations: An Introduction to  
47  
48  
49  
50  
51  
52  
53  
54  
55  
56  
57  
58  
59  
60

1  
2  
3 Fractional Derivatives, Academic Press, San Diego, CA, (1998).

4 [18] N. Alibaud, P. Azerad, D. Isèbe, A non-monotone nonlocal conservation law for  
5 dune morphodynamics, Differential and integral equations, 23 (2010) 155-188.

6 [19] Q. Fei, A. Li, X. Han, C. Miao, Modal identification of long-span Runyang Bridge  
7 using ambient responses recorded by SHMS, Science in China Series E: Technological  
8 Sciences, 52 (2009) 3632.

9 [20] Y. Liu, Investigation on Finite Element Modeling of Long-span Suspension Bridge  
10 for Structural Health Monitoring, Southeast University, Nanjing, 2005.

11 [21] J. Wang, Establishment of Original Fingerprint Databank of Runyang Bridge over  
12 Yangtze River, TongJi University, Shanghai, 2006.

13  
14  
15  
16  
17  
18  
19  
20  
21  
22  
23  
24  
25  
26  
27  
28  
29  
30  
31  
32  
33  
34  
35  
36  
37  
38  
39  
40  
41  
42  
43  
44  
45  
46  
47  
48  
49  
50  
51  
52  
53  
54  
55  
56  
57  
58  
59  
60

Accepted Manuscript